Mon. Not. R. astr. Soc. (1989) **238,** 357–378

CCD surface photometry of radio galaxies – I. FR class I and II sources

Frazer N. Owen★ *National Radio Astronomy Observatory,† Socorro, New Mexico 87801, USA*

Robert A. Laing★ *Royal Greenwich Observatory, Herstmonceux Castle, Hailsham, East Sussex BN27 1RP*

Accepted 1988 November 23. Received 1988 November 21; in original form 1988 May 27

Summary. CCD surface photometry of 47 radio galaxies in the *R*-band is reported. The goal of the programme is to study the relationship of the properties of the parent galaxies to the radio structure and, in particular, to look for differences between Fanaroff & Riley (FR) class I and II sources. In order to clarify some ambiguous cases in the FR classification, we define Classical Double, Twin Jet and Fat Double sources. We describe our definitions of these three classes and their relation to the FR classification. We then show that Classical Double sources are generally associated with normal giant elliptical galaxies with absolute magnitudes near M^* of the Schechter luminosity function and are mostly considerably fainter than first-rank galaxies in rich clusters. Twin Jet and Fat Double sources, on the other hand, are associated with brighter galaxies. These galaxies are also larger and have flatter optical brightness distributions than most giant ellipticals. They can generally be described, following Mathews, Morgan & Schmidt, as D or cD galaxies. These results imply that Classical Doubles (FR II) with $P_{1400} \lesssim 3 \times 10^{26}$ W Hz^{-1} cannot normally evolve into Twin Jet (FR I) sources, since the two classes are associated with different types of galaxies. We suggest that Classical Doubles are essentially transient, whereas Twin Jet sources are more stable, with longer lifetimes.

1 Introduction

While great efforts have been made to image radio galaxies with the VLA and other synthesis instruments, relatively little optical surface photometry of the parent galaxies has been reported. Mathews, Morgan & Schmidt (1964) described the optical forms of galaxies associated with radio sources and originated the N, D and cD classifications (following Morgan

★Visiting Astronomer at NOAO, operated by the Association of Universities for Research in Astronomy, Inc., under contract with the National Science Foundation.

†The National Radio Astronomy Observatory is operated by Associated Universities, Inc., under contract with the National Science Foundation.

1958). They stressed that radio galaxies are elliptical-like systems, albeit often with bright nuclei, extended envelopes or other unusual structures. There are still very few exceptions to this rule, at least over the redshift range for which detailed observations are possible. A few radio galaxies have clear stellar discs (e.g. Sansom *et al.* 1987) and others are severely distorted (Heckman *et al.* 1986), but even these have light distributions which are dominated by an elliptical component. Also some of the most distant radio galaxies may be qualitatively different in structure (McCarthy *et al.* 1987). The only recent extensive optical study of radio galaxies was that by Lilly, McLean & Longair (1984) and Lilly & Prestage (1987), who presented photometric parameters for 45 galaxies and discussed their relation to radio structure, nuclear emission and clustering environment.

In most studies of radio galaxies, it is simply assumed that all radio galaxies are bright elliptical galaxies with absolute magnitudes $M_V \approx -22.0 \pm 0.5$ for $H_0 = 75$ km s^{-1} Mpc^{-1} (e.g. Kron, Koo & Windhorst 1985). It is often supposed that giant cD galaxies in the centres of rich clusters and relatively isolated radio galaxies are similar objects. This paper and paper II in this series (Owen & White, in preparation) examine whether or not these assumptions are correct.

The optical properties of radio galaxies are expected to be closely related to the physics of the radio emission. In particular, the optical light distribution acts as a tracer of the gravitational potential, which in turn determines the distribution of gas around the radio source. The depth and shape of the potential may affect the luminosity and structure of the radio source by controlling both the fuelling rate of the active nucleus and the distribution of confining pressure. The fraction of galaxies of a particular type which are associated with radio sources constrains the duty cycle of radio activity. Also, it has been occasionally proposed that powerful radio sources evolve into weak ones, in which case both classes should be associated with the same type of optical galaxy. We have set out to study these problems by carrying out CCD surface photometry of radio galaxies.

In Section 2 we discuss the choice of the sample and the observing procedures. In Section 3 we review the reduction procedures and present the results of our photometry. In Section 4 we discuss a modification (or clarification) of the standard FR I/FR II classification scheme for radio structure and analyse our photometry in terms of this system. Section 5 is a discussion of the theoretical implications of our results for both the physical picture of the radio sources and their evolution. Section 6 is a summary of our conclusions.

2 Observations

2.1 CHOICE OF THE SAMPLE

Our aim was to probe the relationship of the radio structures of galaxies to their optical profiles. We started with the 3CR sample as documented by Laing, Riley & Longair (1983). Since the lower redshift objects are easier to study due to their larger scale (arcsec kpc^{-1}), only objects with redshifts less than 0.2 have been selected. These objects also tend to have the highest-quality radio maps and to have been studied fairly thoroughly, although the number with high-quality maps and redshifts even in this sample is smaller than one would like. In some cases the number of objects of a particular morphological type is very low; also a number of interesting objects are near to bright stars which make the study of their surface brightness distributions difficult. For these reasons, we have added a number of objects from other surveys in order to fill out our sample. Thus the sample is not complete but has been chosen to allow us to explore the dependence of optical surface brightness on radio properties as fully as possible in a small sample.

2.2 OBSERVING PROCEDURES

The observations were made using the #1 RCA CCD direct camera on the #1 0.9-m $f/7.5$ telescope at Kitt Peak. The RCA CCD with this configuration has a pixel size of 30 μm and an overall size of 512×320 pixels yielding a field of view 7.3 arcmin in RA by 4.6 arcmin in declination. The pixel scale is 0.86 arcsec. All of the observations reported in this paper used an RG 610 (R-band) filter. This camera and filter system are described by Davis *et al.* (1985). Exposure times were usually 2000 s, typically yielding 15 000 detected electrons (or photons) from the sky in each pixel, equivalent to a Poisson counting noise of about 120 electrons. The readout noise was about 75 electrons; thus for an integration of about 750 s the readout noise and the Poisson sky noise are equal. Therefore for most of our integrations our noise is dominated by the sky noise but not by a very large factor. 2000 s was the longest observing time practicable to avoid exceeding the upper bound for linear operation of the CCD for some parts of the galaxy. For some galaxies the cores were too bright to avoid saturation with 2000 s integration times; then shorter integration times were used and several scans were stacked if necessary.

2.3 FINAL OBSERVING LIST

The final observing list and its associated parameters are given in Table 1. Column 1 contains the most commonly used source name and column 2 the IAU name; in columns 3 and 4 we list the UT date of the observation and the integration time in seconds; column 5 gives the redshift of the source and column 6 our classification of the source structure (TJ: Twin Jet, CD: Classical Double, FD: Fat Double: see Section 4.3 for a discussion of the source classifications).

3 Reductions

3.1 PHOTOMETRIC CALIBRATION

Standard calibrations for dc and pixel-to-pixel bias variations, and quantum efficiency were made using the KPNO mountain software as described by Davis *et al.* (1985). After correction for the sensitivity variations using exposures of a white screen illuminated by a tungsten lamp, the frames were typically flat to 1 per cent, although a small linear gradient along one of the axes of the chip across the entire face of the frame was sometimes visible. This effect was minimized by subtracting images of tilted planes (either in RA or declination) from each frame. The final gradient was usually reduced in this manner to 0.1 to 0.3 per cent peak-to-peak across the frame.

Photometric calibration of the extinction and transformation to the Cousins R_C scale were made each night by observing ten to twenty standard stars from the equatorial catalogue of Landolt (1983), using a list of these stars and their magnitudes on the Cousins scale provided by KPNO. For the R filter described above we found no scale transformation necessary to the Cousins scale to an accuracy of about one per cent. Thus each night we determined two constants, namely the system zero point and the extinction. Typical rms errors in the fitted extinction curves were 0.02 to 0.03 mag on good nights. If the standard stars revealed that part or all of the night was bad (or it appeared from the sky that the night was questionable), we re-observed the field with a short exposure on a good night to establish the calibration.

Comparison of our photometry with aperture photometry by Sandage (1973), after transformation to the Cousin's scale for 12, supposedly non-variable objects, yields an rms difference between the two sets of data of 0.08 mag and no detectable systematic difference. We thus believe the overall rms error in our photometry to be $\lesssim 0.05$ mag.

Table 1. Observed sample.

Source Name	I.A.U. Name	Obs. Date	Integration Time (Sec)	Redshift	Morph. Type	FR Class	Ref. O	Ref. R
3C31	0104+321	01Nov83	2000	0.0167	TJ	1	7	36
3C33	0106+130	01Nov83	2000	0.0595	CD	2	1	25
3C61.1	0210+860	01Nov83	2000	0.186	CD	2	40	25
VV7.08.14	0326+396	25Mar85	3×300	0.0243	TJ	1	11	38
3C98	0356+102	24Mar85	2000	0.0306	CD	2	1	27
3C111	0415+379	24Mar85	2000	0.0485	CD	2	3	4
3C120	0430+052	23Mar85	500	0.0334	Core	1	39	5
3C135	0511+008	26Mar85	2000	0.1273	CD	2	7	6
0712+534	0712+534	25Mar85	2000	0.064	FD	1/2	8	9
3C184.1	0734+805	23Mar85	2000	0.1182	CD	2	7	27
DA240	0745+560	30Oct83	2000	0.0356	FD	1/2	39	41
NGC2484	0755+379	24Mar85	2×1000	0.0433	FD	1	11	13
3C192	0802+243	27Mar85	1500	0.0598	CD	2	7	25
0816+526	0816+526	26Mar85	2000	0.189	CD	2	12	24
3C197.1	0818+472	27Mar85	2000	0.1301	CD	2	12	12
0915+320	0915+320	25Mar85	2000	0.0620	TJ	1	42	13
Hydra A	0915−118	28Mar85	600	0.0650	TJ	1	1	14
3C219	0917+458	25Mar85	2000	0.1744	CD	2	1	15
3C223	0936+361	28Mar85	2000	0.1368	CD	2	7	27
3C223.1	0938+399	23Mar85	2000	0.1075	CD	2	7	10
3C227	0945+076	23Mar85	2000	0.0861	CD	2	7	16
4C73.08	0945+734	24Mar85	2000	0.0581	CD	2	44	17
3C234	0958+290	25Mar85	2000	0.1848	CD	2	1	10
3C236	1003+351	15May83	2000	0.0989	CD	2	7	29
NGC3121	1004+146	23Mar85	1000	0.0296	TJ	1		18
1017+487	1017+487	26Mar85	2000	0.053	CD	2	8	9
1205+341	1205+341	23Mar85	2000	0.0788	CD	2	19	19
1232+414	1232+414	24Mar85	2000	0.191	CD	2	12	10
NGC5127	1321+318	24Mar85	1000	0.0161	TJ	1	11	37
NGC5141	1322+366	28Mar85	600	0.0174	TJ	1	11	30
3C293	1350+316	24Mar85	2×1000	0.0452	TJ	1	11	20
NGC5490	1407+177	24Mar85	2×500	0.0163	TJ	1		18
3C296	1414+110	23Mar85	1000	0.0237	TJ	1	7	21
3C303	1441+522	23Mar85	2000	0.141	CD	2	7	25
1455+287	1455+287	23Mar85	2000	0.1411	CD	2	19	13
3C310	1502+262	24May85	2000	0.0540	FD	1/2	1	22
3C315	1511+263	23Mar85	2000	0.1083	CD	2	1	22
3C319	1522+546	25Mar85	2000	0.192	CD	2	2	22
3C326	1549+242	27Mar85	2000	0.0895	CD	2	7	31
NGC6251	1637+826	17May83	2000	0.0234	TJ	1/2	43	34
Herc A	1648+050	27Mar85	1000	0.154	TJ	1/2	1	23
3C371	1807+698	23Mar85	6×300	0.050	Core	1	7	33
3C382	1833+326	27Mar85	6×300	0.0578	CD	2	19	32
3C388	1842+455	24Mar85	2000	0.0908	FD	2	1	24
3C390.3	1845+797	24Mar85	4×300	0.0569	CD	2	7	27
Cygnus A	1957+405	24Apr85	7×600	0.0570	CD	2	1	26
3C449	2229+390	02Nov83	2000	0.0171	TJ	1	7	35

(refs for table 1)

(1) Griffin 1963; (2) Jenkins, Pooley & Riley 1977; (3) Longair & Gunn 1975; (4) Linfield & Perley 1984; (5) Walker, Benson & Unwin 1987; (6) Laing & Owen 1989; (7) Wyndham 1966; (8) Burns & Owen 1979; (9) Burns & Gregory 1982; (10) Burns *et al.* 1984; (11) Colla *et al.* 1975; (12) Rudnick & Owen 1977; (13) de Ruiter *et al.* 1986; (14) Simkin & Ekers 1983; (15) Perley *et al.* 1980; (16) Baum *et al.* 1989; (17) Mayer 1979; (18) Jenkins 1982; (19) Fanti *et al.* 1978; (20) Bridle, Fomalont & Cornwell 1981; (21) Birkinshaw, Laing &

Peacock 1981; (22) Leahy & Williams 1984; (23) Dreher & Feigelson 1984; (24) Burns & Christiansen 1980; (25) Laing 1981; (26) Perley, Dreher & Cowan 1984; (27) Miller 1985; (28) Alexander 1985; (29) Barthel *et al.* 1985; (30) Fanti *et al.* 1986; (31) Willis & Strom 1978; (32) Antonucci 1985; (33) Ulvestad & Johnston 1984; (34) Bridle & Perley 1984; (35) Cornwell & Perley 1985; (36) Fomalont *et al.* 1980; (37) Fanti *et al.* 1982; (38) Parma 1982; (39) Caswell & Wills 1967; (40) Gunn *et al.* 1981; (41) Willis *et al.* 1974; (42) Fanti *et al.* 1973; (43) Waggett *et al.* 1977; (44) Demoulin 1970.

3.2 DATA ANALYSIS

The fully calibrated and flattened frames were analysed for surface brightness profiles using the GASP software developed by Michael Cawson. The techniques we used and their accuracy are described by Davis *et al.* (1985). As they discuss, all of the confusing images on the CCD frame are first blanked out by a combination of manual and automatic editing routines. The final routine in GASP, PROF, is then used to fit six parameter sets of elliptical isophotes to the galaxy surface-brightness distribution. These fitted curves can then be reduced to five one-dimensional curves for surface brightness, ellipticity, position angle, and x-centre and y-centre of each ellipse as a function of the major axis of the ellipse.

These one-dimensional curves were further analysed to derive basic information about the parent galaxies. First, in order to study the shape of the profiles, two functions were fitted to the profiles of surface brightness versus radius: a de Vaucouleurs $r^{1/4}$ law and a power law. The fits were made from a radius of 4 arcsec (about four seeing radii; see Schweizer 1981) out to

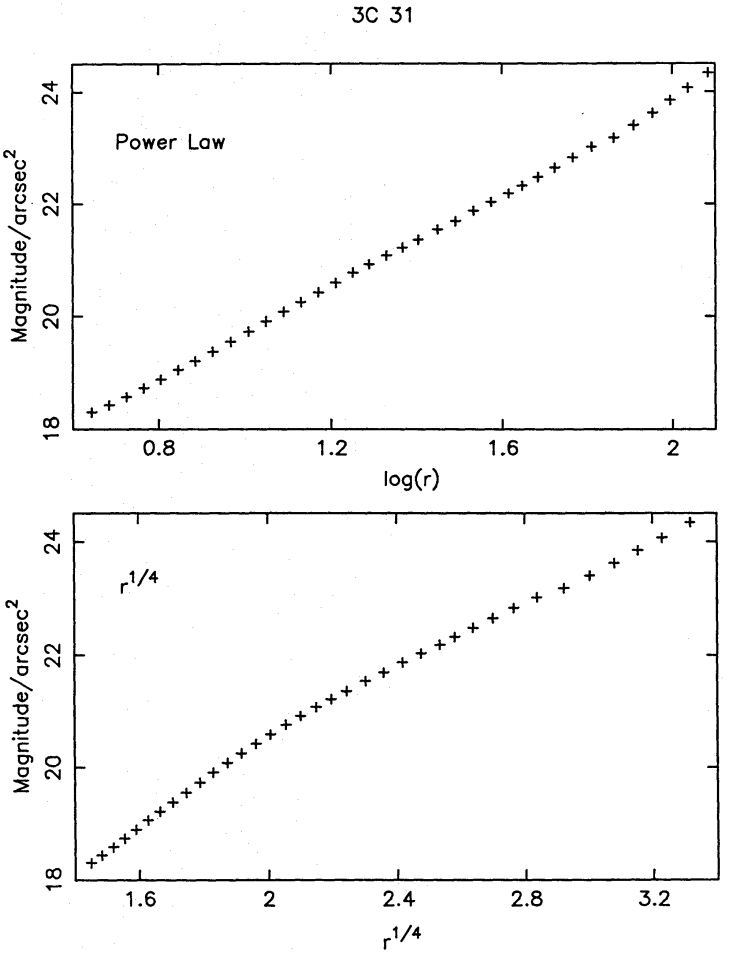

Figure 1. Surface brightness versus radius for 3C31.

24.5 mag arcsec^{-2} in the rest frame of the galaxy as described in the next paragraph. We found that the fits to these profiles were better using $\sqrt{ab}$ as the independent variable, instead of a, where a is the major axis and b is the minor axis. This is an important point since the ellipticity, $1-b/a$, changes significantly with radius for many of the galaxies. Thus, for the rest of this paper we will adopt the radius $r \equiv \sqrt{ab}$.

In Figs 1 and 2 we show the one-dimensional brightness profiles derived for 3C31 and 3C33 plotted as a function of r as defined above. The brightness in mag arcsec^{-2} has been plotted against log r in the upper panel and against $r^{1/4}$ in the lower panel, so that in the upper panel a power law and in the lower panel a de Vaucouleurs law would be a straight line. 3C31 is most consistent with a power law while 3C33 fits a de Vaucouleurs law best, but one can see that the differences from the theoretical curves are small, and most of the systems reported in this paper can be described crudely by either law over the range of brightness studied.

We have also derived isophotal magnitudes and sizes for each galaxy for an isophote of 24.5 mag arcsec^{-2} *in the rest frame of the galaxy.* This means that, before we have picked the isophotal limit to which the profile is to be summed, we have corrected for K-dimming and for galactic absorption. We have then also made K-corrections and a galactic absorption correction to the total magnitudes. The galactic absorption corrections were made using the reddening estimates of Burstein & Heiles (1982). The surface brightness correction for the redshift range we have studied ($\lesssim 0.2$) was approximated as $\Delta B = (1+z)^4$ mag arcsec^{-2}. Similarly, the

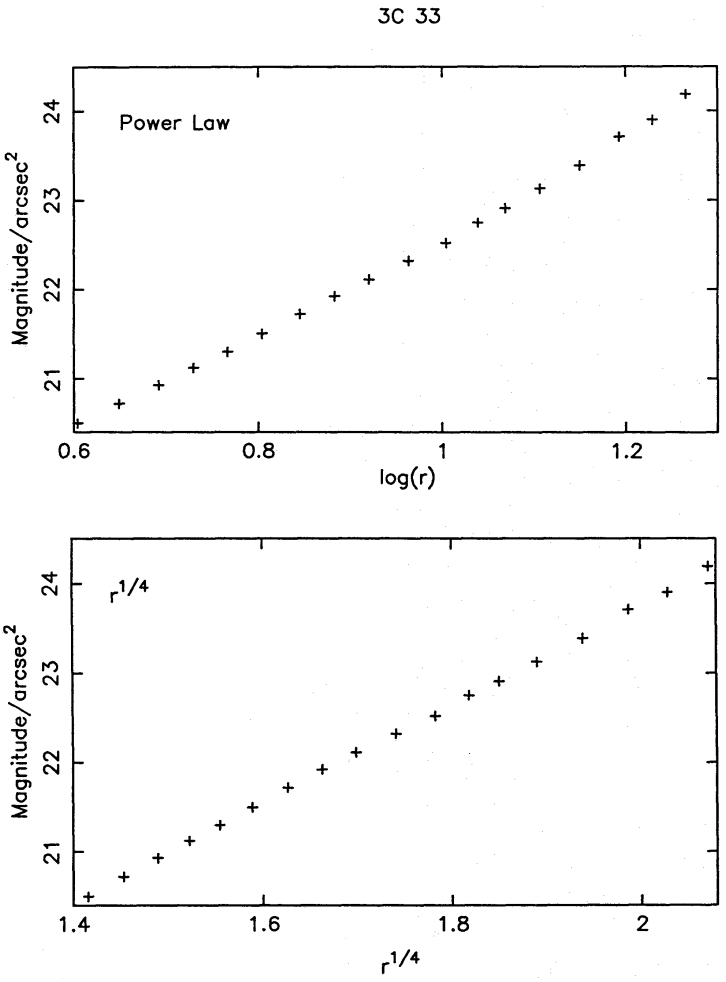

Figure 2. Surface brightness versus radius for 3C33.

K-correction to the total magnitude was approximated as $\Delta M = -(1+z)^2$. For all absolute magnitude calculations, we assumed $H_0 = 75$ km s^{-1} Mpc^{-1} and $q_0 = 0$.

Finally, we calculated (Sandage 1972; Gunn & Oke 1975) metric magnitudes using the AIPS data analysis system. Table 2 summarizes the apparent and absolute magnitudes. In columns 2–4 we give the apparent magnitudes for the Gunn-Oke, Sandage and R(24.5)

Table 2. Total magnitudes.

Source Name	Apparent Magnitude G-O	S	$m_{24.5}$	Absolute Magnitudes G-O	S	$M_{24.5}$
3C31	11.47	10.90	11.11	-22.76	-23.33	-23.12
3C33	14.89	14.65	14.80	-22.15	-22.39	-22.24
3C61.1	18.55	17.60	18.43:	-21.27	-22.22	-21.39:
0326+396	12.78	11.41	12.74	-22.55	-23.92	-22.59
3C98	14.08	13.54	14.18	-21.65	-22.19	-21.55
3C111	17.20	16.51	17.32	-20.61:	-21.30:	-20.47:
3C120	13.54	13.39	13.54	-22.44	-22.59	-22.44
3C135	16.77	16.22	16.76	-22.18	-22.73	-22.19
0712+534	14.20	13.44	13.22	-23.06	-23.82	-24.04
3C184.1	17.17	17.07	17.21	-21.44	-21.54	-21.40
DA240	13.79	13.51	13.71	-22.06	-22.34	-22.14
NGC2484	13.25	12.75	12.59	-23.09	-23.59	-23.75
3C192	15.16	14.30	15.20	-21.90	-22.76	-21.86
0816+526	18.30	17.79	17.94	-21.44	-21.95	-21.80
3C197.1	16.88	16.58	16.76	-21.98	-22.28	-22.10
0915+320	14.70	14.30	14.40	-22.43	-22.83	-22.73
Hydra A	14.18	13.60	13.23:	-23.07	-23.65	-24.02:
3C219	16.89	16.16	16.20	-22.60	-23.33	-23.29
3C223	16.94			-22.02		
3C223.1	16.06	15.85	16.01	-22.32	-22.53	-22.37
3C227	15.80	15.52	15.81	-22.04	-22.32	-22.03
4C73.08	14.91	14.56	14.74	-22.06	-22.41	-22.23
3C234	17.59	17.07	17.24	-22.07	-22.59	-22.42
3C236	16.14	15.57	15.36	-22.06	-22.63	-22.84
NGC3121	12.64	12.24	12.32	-22.80	-23.20	-23.12
1017+487	14.99	14.41	14.96	-21.73	-22.34	-21.79
1205+341	15.26	15.02	15.17	-22.36	-22.60	-22.45
1232+414	17.30	16.98	17.06	-22.43	-22.75	-22.67
NGC5127	12.08	11.74	11.93	-21.99	-22.14	-22.14
NGC5141	12.34	11.49	12.36	-21.91	-22.76	-21.89
3C293	14.02	13.64	13.72	-22.34	-22.72	-22.64
NGC5490	11.74	11.34	11.65	-22.38	-22.78	-22.47
3C296	11.82	11.35	11.43	-23.13	-23.60	-23.52
3C303	16.66	16.24	16.29	-22.37	-22.79	-22.74
1455+287	16.55	16.20	16.35	-22.47	-22.82	-22.67
3C310	14.69	12.42	13.92	-22.12	-24.39	-22.89
3C315	16.18	15.65	16.16	-22.24	-22.77	-22.32
3C319	18.22	17.81	18.07	-21.55	-21.96	-21.70
3C326	16.46	16.11	15.72	-21.51	-21.86	-22.26
NGC6251	12.30	11.86	11.66	-22.78	-23.22	-23.42
Herc A	16.97	16.21	15.89	-22.36	-23.12	-23.44
3C371	13.69	13.53	13.59	-23.00	-23.16	-23.10
3C382	13.63	13.43	13.58	-23.52	-23.72	-23.57
3C388	14.95	14.33	14.12	-23.10	-23.72	-23.93
3C390.3	14.75	14.55	14.64	-22.21	-22.41	-22.32
Cygnus A	14.47			-23.13		
3C449	12.50	12.00	12.35	-22.00	-22.50	-22.15

systems; in columns 5–7 we list the associated absolute magnitudes. In Table 3 we summarize the photometric structural information obtained for each radio galaxy. In columns 2 and 3 we give the rms found for the power law and $r^{1/4}$ law fits to surface brightness profiles, respectively (in magnitudes); the number of points used in the fit is given in column 4; in columns 5 and 6 we list the exponent for the best-fitting power law and the equivalent radius (in kpc) found from the $r^{1/4}$ law fit; in columns 7, 8 and 9 the position angle, ellipticity and radius (in kpc) are given for the 24.5 mag arcsec^{-2} isophote.

Table 3. Photometric structure parameters.

Source	σ_{PL}	$\sigma_{r^{1/4}}$	Points	PL exp.	r_e	$\theta_{24.5}$	$\epsilon_{24.5}$	$r_{24.5}$
3C31	0.047	0.181	36	-1.65	14.8	138	0.17	39.9
3C33	0.093	0.043	19	-2.25	4.9	150	0.23	20.3
3C61.1						35	0.30:	14.6:
0326+396	0.130	0.068	31	-1.89	8.4	45	0.24	26.9:
3C98	0.078	0.063	20	-2.11	4.1	50	0.15	15.3
3C111	0.131	0.141	13	-1.69	10:	160	0.2	9.9
3C120	0.148	0.094	23	-1.86	7.9	118	0.27	19.4
3C135	0.098	0.128	10	-2.92	2.6	60	0.15	22.9
0712+534	0.075	0.093	34	-1.60	40.3	138	0.6	70.6
3C184.1	0.028	0.017	10	-2.91	1.4	38	0.4	11.0
DA240	0.149	0.065	24	-2.00	6.1	35	0.25	20.3
NGC2484	0.131	0.067	32	-1.74	20.0	145	0.45	49.3
3C192	0.120	0.067	16	-2.40	3.2	140	0.08	16.3
0816+526	0.052	0.042	11	-1.98	13.5	85	0.34	21.8
3C197.1	0.031	0.024	11	-2.56	3.8	85	0.3	20.6
0915+320	0.099	0.041	23	-1.91	11.4	0	0.5	29.1
Hydra A	0.094	0.050	24	-1.58	30.0	50	0.3:	67:
3C219	0.075	0.059	17	-1.62	35.8	30	0.5	38.0
3C223	0.034	0.029	12	-2.04	9.7			
3C223.1	0.054	0.049	12	-2.77	2.7	25	0.27	19.4
3C227	0.053	0.034	13	-2.34	4.4	170	0.15	16.8
4C73.08	0.084	0.069	21	-2.07	7.4	30	0.2	24.4
3C234	0.032	0.020	10	-2.46	5.6	111	0.54	24.0
3C236	0.061	0.037	19	-2.01	12.1	55	0.35	33.1
NGC3121	0.094	0.030	18	-2.10	10.1	0	0.15	32.1
1017+487	0.026	0.052	16	-1.85	6.1	70	0.25	17.8
1205+341	0.123	0.059	16	-2.48	3.8	20	0.08	21.4
1232+414	0.045	0.055	11	-2.44	6.0	140	0.25	25.0
NGC5127	0.182	0.041	32	-1.73	8.5	74	0.3	22.7
NGC5141	0.145	0.052	28	-2.04	3.8	71	0.3	16.4
3C293	0.182	0.102	25	-2.02	8.0	65	0.5	28.2
NGC5490	0.153	0.069	32	-1.93	5.5	10	0.2	21.7
3C296	0.127	0.057	32	-1.78	11.9	150	0.14	37.8
3C303	0.029	0.046	15	-1.94	15.8	174	0.22	30.2
1455+287	0.102	0.070	11	-2.69	3.4	165	0.2	23.7
3C310	0.147	0.072	29	-1.42	42.3	90	0.4	41.7
3C315	0.170	0.137	15	-1.92	12.8	25	0.3	24.6
3C319	0.055	0.050	11	-1.72	20.4	135	0.23	18.6
3C326	0.084	0.044	18	-2.00	10.2	152	0.5	23.7
NGC6251	0.023	0.192	37	-1.68	18.2	15	0.25	48.4
Herc A	0.090	0.041	19	-1.88	21.3	117	0.5	47:
3C371	0.042	0.129	24	-1.91	10.5	65	0.2	27.8
3C382	0.139	0.077	20	-2.32	4.7	75	0.2	24.3
3C388	0.100	0.030	28	-1.73	28.1	55	0.5	57.0
3C390.3	0.036	0.045	15	-2.04	5.9	110	0.15	16.6
3C449	0.092	0.263	40	-1.62	14.4	70	0.65	31.3

4 Analysis

4.1 SELECTION OF THE SAMPLE TO BE ANALYSED

The sample described in Tables 1–3 was picked to cover a wide range of radio structure and luminosity. In order to study it statistically we require a subsample with well-defined and determined properties. We exclude (i) the two objects with luminosities below 10^{24} W Hz^{-1} at 1400 MHz (NGC 5127 and 5490); (ii) objects with $|b|<10°$, since they have poorly known galactic absorption (e.g. 3C111) and they are often in crowded star fields which make surface photometry difficult (e.g. Cygnus A), and (iii) three objects with dominant radio and/or optical cores (3C120, 3C371, and 3C382) since such objects are not adequately represented in our sample and in such cases the contribution of the optical core makes the surface photometry of the starlight difficult.

4.2 THE CORRELATION OF ABSOLUTE MAGNITUDE AND RADIO PROPERTIES

The first property that one might try to correlate with absolute optical magnitude is the radio luminosity, expecting to find a positive correlation between radio and optical luminosity, and in Fig. 3 we plot radio luminosity at 1400 MHz versus $M_{24.5}$ for our statistical sample as given in Table 2. Little if any correlation is seen in this figure between radio and optical absolute luminosity, although the Fanaroff & Riley classes (see caption) fall generally in separate areas of the diagram.

The Fanaroff & Riley (1974) morphological classification describes radio sources as FR I if the sources are edge-darkened, with the surface brightness of the source highest in the centre and decreasing away from the nucleus, while FR II sources are edge-brightened – faint in the centre and brightest at their maximum distance from the nucleus. Fanaroff & Riley showed that

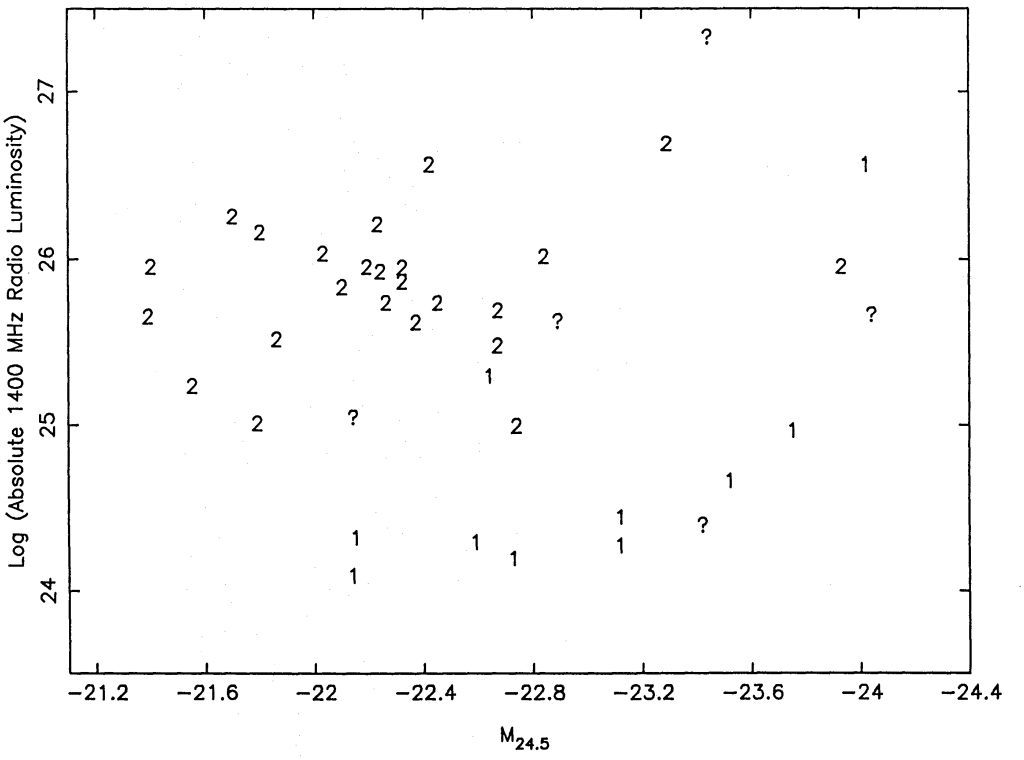

Figure 3. The log of the absolute radio luminosity at 1400 MHz (W Hz^{-1}) versus $M_{24.5}$. Fanaroff & Riley classes are plotted as 1:I, ?:I/II, and 2:II.

most FR I sources have luminosities below 10^{25} W Hz^{-1} at 1400 MHz while most FR II sources are above 10^{25} W Hz^{-1}. From Fig. 3 this is also seen to be the case for our sample but the figure also suggests that galaxies associated with FR II sources tend to be fainter than those associated with FR I sources. In Fig. 4 we show a histogram of the FR I and FR II sources in our statistical sample. From a Wilcoxon rank test between the FR I and FR II subsamples we find that the probability that they originate from the same parent distributions is less than one per cent. This result agrees with the result of Lilly & Prestage (1987) on an almost completely independent sample.

4.3 CLASSIFICATION OF RADIO SOURCE STRUCTURE

The result from the previous section leads us to ask whether there is some better way to classify the radio structures which might also tell us something about the underlying physics.

Our examination of the best maps available suggests the following three-part classification.

(i) Twin Jet sources: Sources whose overall structure can be described by symmetric jets originating in the nucleus and extending on both sides of the radio galaxy. These sources generally fit into the FR I class.

(ii) Classical Double sources: Sources with compact outer hotspots and elongated, diffuse lobes extending from the hotspots back toward the nucleus. These sources are always put in the FR II class.

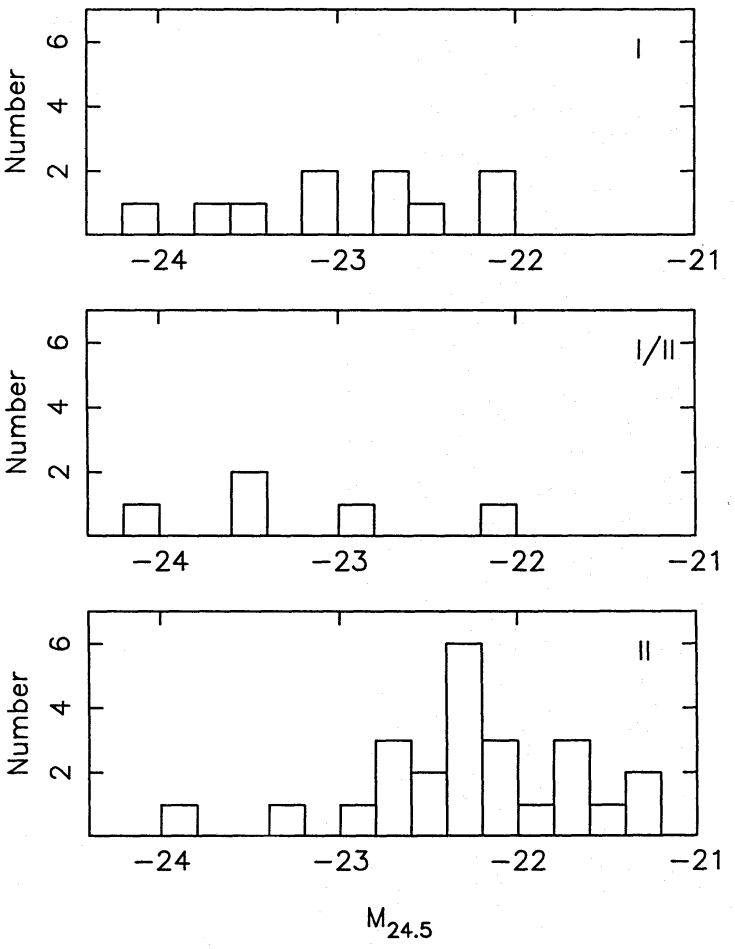

Figure 4. Histograms of $M_{24.5}$ for FR I, FR I/II and FR II sources.

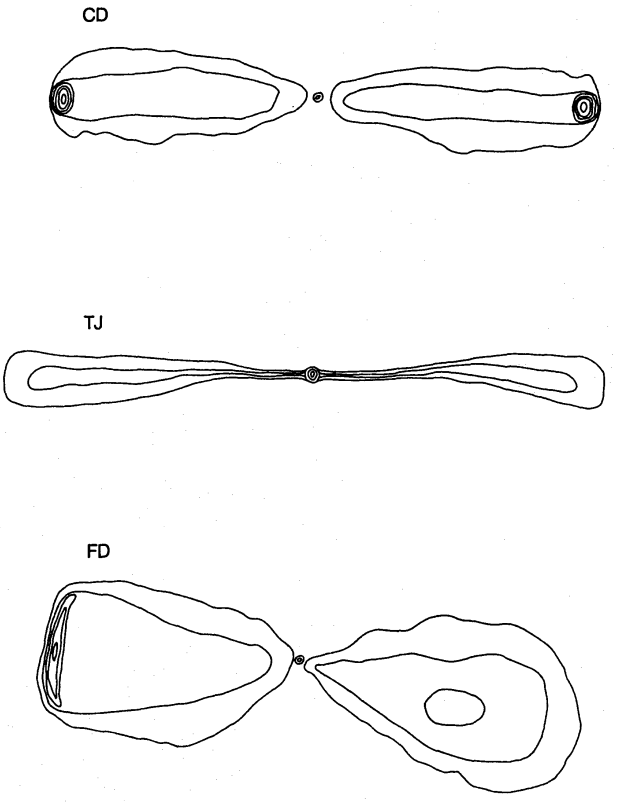

Figure 5. Example sketch of CD, TJ and FD morphological classes.

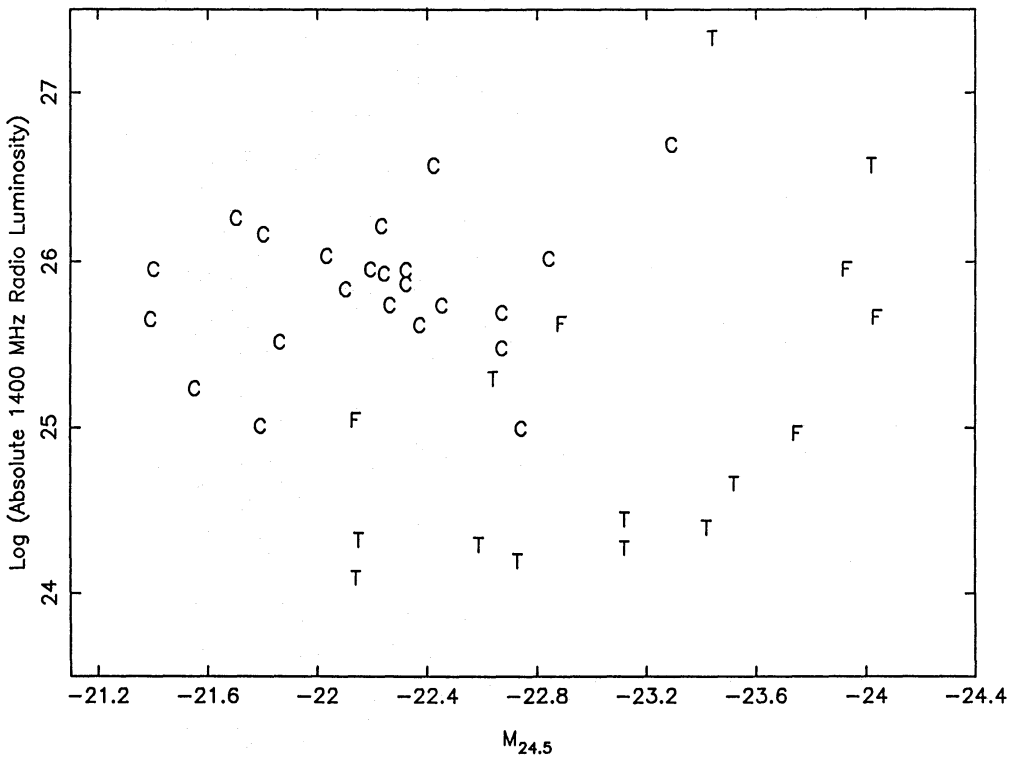

Figure 6. The log of the absolute radio luminosity at 1400 MHz (W Hz^{-1}) versus $M_{24.5}$. CD sources are plotted as C, TJ as T and FD as F.

(iii) Fat Double sources: Sources with bright outer rims of radio emission and roundish diffuse radio lobes. These sources are usualy called FR II or FR I/II. As we discuss below, their optical properties suggest that these sources may really belong with the FR I sources.

In Fig. 5 we show free-hand sketches of the three classes and, in Fig. 6, we plot optical versus radio luminosity for this classification for comparison with Fig. 3.

The main motivation for this classification is the ambiguous nature of the fat double sources in the FR I/II scheme. These sources seem to us likely to be physically different. A few sources, such as Hercules A and NGC 6251, appear in the TJ class instead of calling them a borderline FR I/II. We will discuss our sample in terms of this classification but further work is necessary to demonstrate its validity. In this paper (and paper II) we will compare the properties of the galaxies associated with our three classes and try to establish their proper place in the FR classification.

4.4 SOURCE STRUCTURE VERSUS PHOTOMETRIC PROPERTIES

Figs 7, 8 and 9 contain histograms of the Gunn–Oke, Sandage and $M_{24.5}$ absolute magnitudes from Table 2 versus morphological type. For the Gunn–Oke absolute magnitudes, the mean absolute magnitudes are -21.99 ± 0.08 for the CDs, -22.56 ± 0.12, for the TJs and -22.69 ± 0.24 for the FDs. For the Sandage magnitudes, the means are -22.45 ± 0.08,

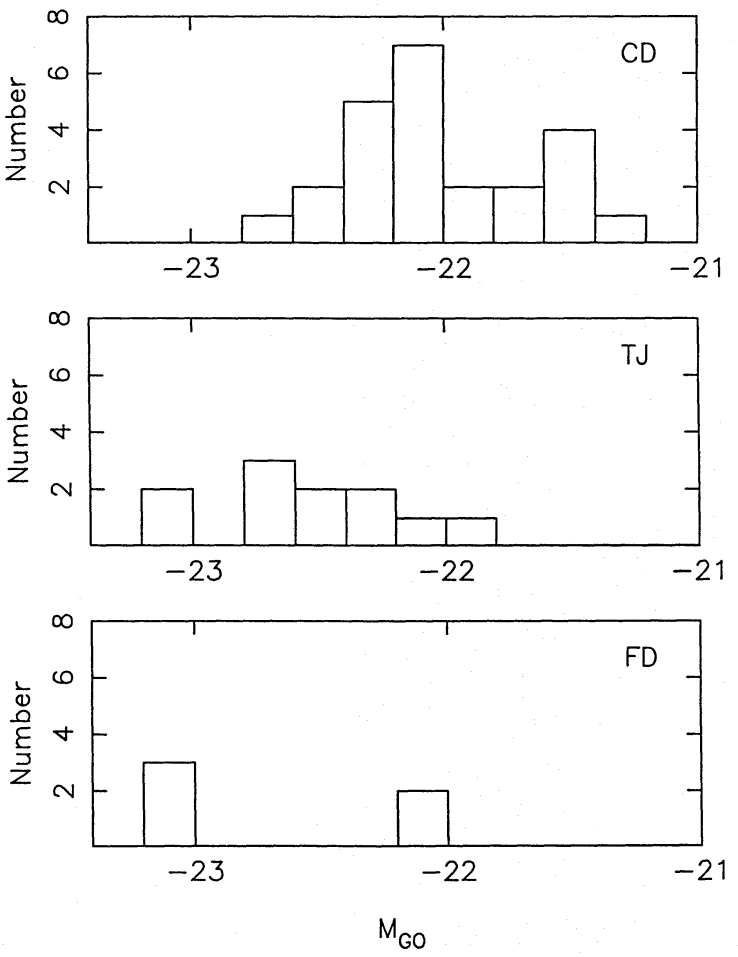

Figure 7. Histograms of Gunn–Oke absolute magnitudes for CD, TJ and FD sources.

-23.11 ± 0.16 and -23.57 ± 0.34, respectively. For $M_{24.5}$, the three means are -22.01 ± 0.10, -22.99 ± 0.18 and -23.35 ± 0.36. For all three types of magnitudes, a Wilcoxon rank test rejects at the 0.2 per cent level the hypothesis that the parent distributions of the CDs and TJs are the same. Comparing the CD and FD distributions, the same test rejects the hypothesis that the parent distributions are the same at the two per cent level for $M_{24.5}$ and Sandage magnitudes, and at the five per cent level for the Gunn–Oke magnitudes. A Kolmogorov–Smirnov test also rejects the hypothesis at the 2 per cent level for the $M_{24.5}$ and Sandage magnitudes but only at the 10 per cent level for the Gunn–Oke magnitudes. Other tests also reject the hypothesis that the TJ and/or the FD sources could be selected from the same sample as the CD sources. Thus we conclude that the galaxies associated with Twin Jet and probably the Fat Double radio sources are statistically brighter than the Classical Double sources. Somewhat surprising, however, is that this result holds for all three types of magnitudes. In other words, the magnitude segregation by radio class is not just due to the outer haloes of the galaxies, although the effect is stronger when the fainter parts of the galaxies are included. Nonetheless, the rms scatter in the magnitudes for each radio class is smallest for the Gunn–Oke magnitudes which use the smallest aperture.

All of the profiles were fitted with de Vaucouleurs $r^{1/4}$ laws and power laws. Table 3 contains the rms of the residuals to both fits, r_e from the $r^{1/4}$ law fits and the exponent for the best power-law fit. Fig. 10 shows histograms of the power-law exponents for the three classes. About 80 per cent of the galaxies fitted $r^{1/4}$ laws better than a power law. (In paper II where we

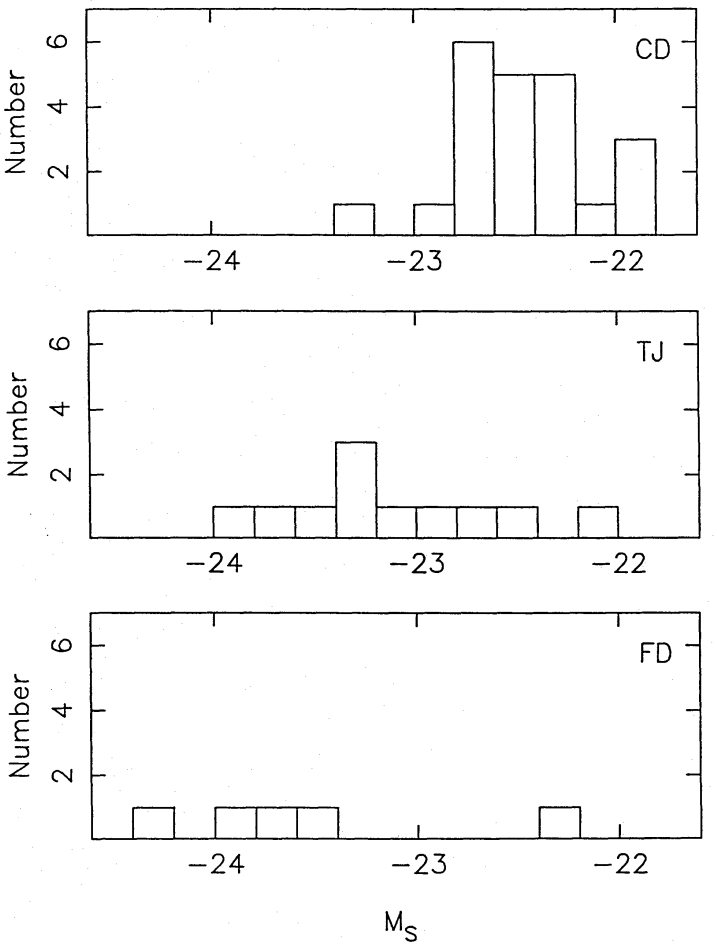

Figure 8. Histograms of Sandage absolute magnitudes for CD, TJ and FD sources.

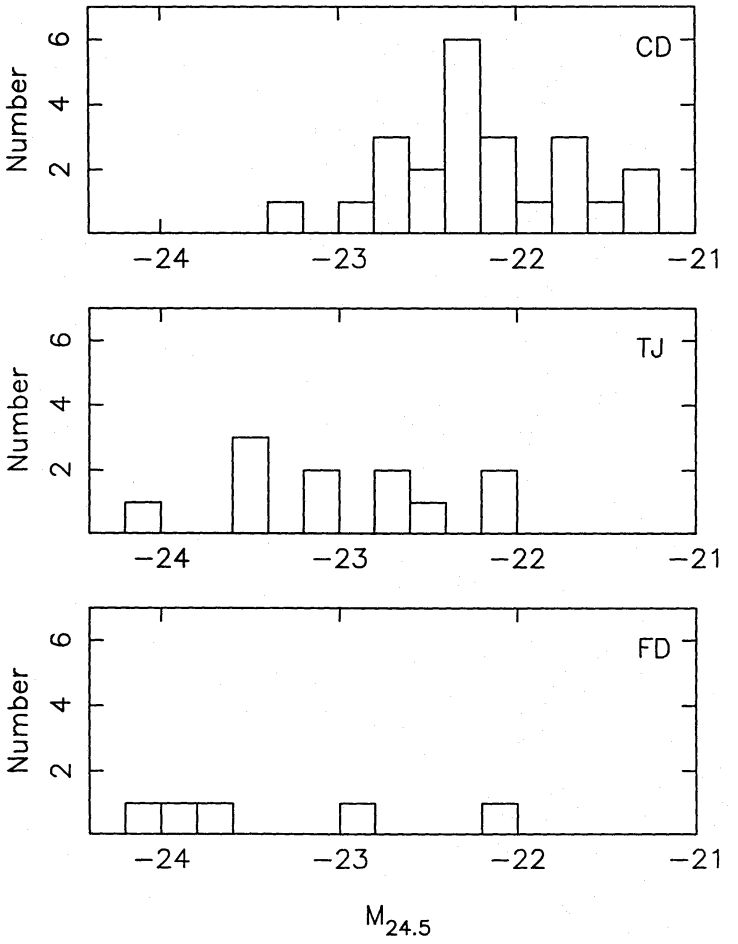

Figure 9. Histograms of $M_{24.5}$ for CD, TJ and FD sources.

consider radio galaxies in Abell clusters, most of the galaxies fit power laws better than $r^{1/4}$ laws.) Three sources fitted power laws much better than $r^{1/4}$ laws, namely 3C31, NGC 6251 and 3C449. These three objects are low-luminosity, TJ, sources. The mean values for the exponents of the best-fitting power laws were -2.25 ± 0.08 for the CDs, -1.80 ± 0.05 for the TJs and -1.70 ± 0.10 for the FDs. A rank test shows that both the TJ and the FD sources have power-law slopes inconsistent with the CD sources at the 0.1 and 0.2 per cent probability level, respectively. This result suggests that the TJ and FD sources have generally flatter light profiles than the CD sources.

In Fig. 11, we present the histograms of r_e from the de Vaucouleurs law fits. The mean values of r_e for the three classes are 8.2 ± 1.7 kpc for the CDs, 14.3 ± 2.0 kpc for the TJs and 27.4 ± 6.7 kpc for the FDs. Once again, rank comparisons of TJ sources with the CD sources and the FDs with the CDs show the distributions to be inconsistent at the 1 per cent level in both cases. Fig. 12 contains the histogram of the isophotal radius at 24.5 mag arcsec^{-2} in the frame of the galaxy. The mean values of $r_{24.5}$ for the three classes are 21.7 ± 1.3 kpc for the CDs, 37.3 ± 3.9 kpc for the TJs and 47.8 ± 8.4 kpc for the FDs. The rank test once again shows that the TJ and CD distributions are inconsistent at the 0.1 per cent level and that the FD and CD distributions are inconsistent at the 1 per cent level. Thus, from both of these size criteria, the TJ and FD galaxies are larger than the CDs.

In Fig. 13, we compare the histograms of the ellipticity of the galaxies at the 24.5 mag arcsec^{-2} isophote. The mean values for $\varepsilon_{24.5}$ are 0.27 ± 0.03 for CDs, 0.34 ± 0.05 for TJs and

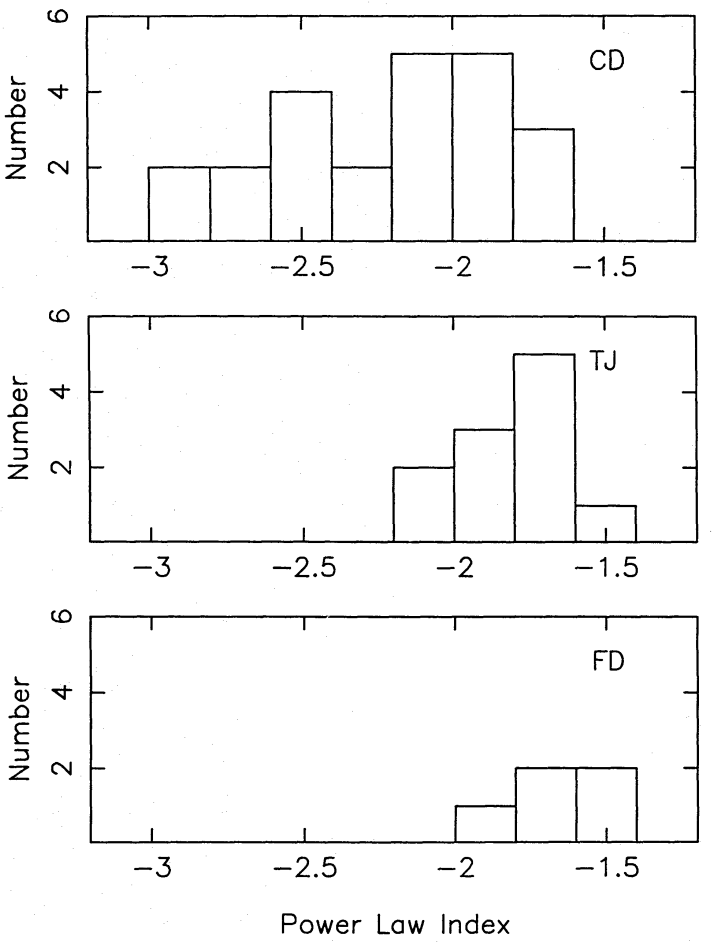

Figure 10. Histograms of the power-law exponents fitted to the one-dimensional brightness profiles for CD, TJ and FD sources.

0.44 ± 0.06 for FDs. A rank test finds no significant difference between the TJ and CD at about the 50 per cent level, while the FD and CD distributions are inconsistent at the 2 per cent level. A Kolmogorov–Smirnov test finds that the FD and CD distributions are not consistent with the same parent distribution at the ten per cent level. Thus the case for any difference in ellipticity is weak.

In summary, there seems to be little evidence for any differences between the TJ and FD galaxies but both of these types of sources seem to be intrinsically brighter, larger, and have flatter light distributions than the CD galaxies. From the evidence in this paper it seems that TJ and FD sources are very similar optically and might be considered as FR I sources, while CD's are clearly FR II sources. However, larger samples of FD sources are needed to clarify this point.

5 Discussion

5.1 CD PARENT GALAXIES

The parent galaxies for the CD radio sources appear generally to be giant elliptical galaxies but not first-rank cluster galaxies. Interestingly, the mean absolute magnitude of -22.01 for the Cousins R-band and $H_0 = 75$ km s^{-1} Mpc^{-1} and $q_0 = 0$ is very close to the best estimates for M^* for the Schechter luminosity function transformed to the same magnitude system

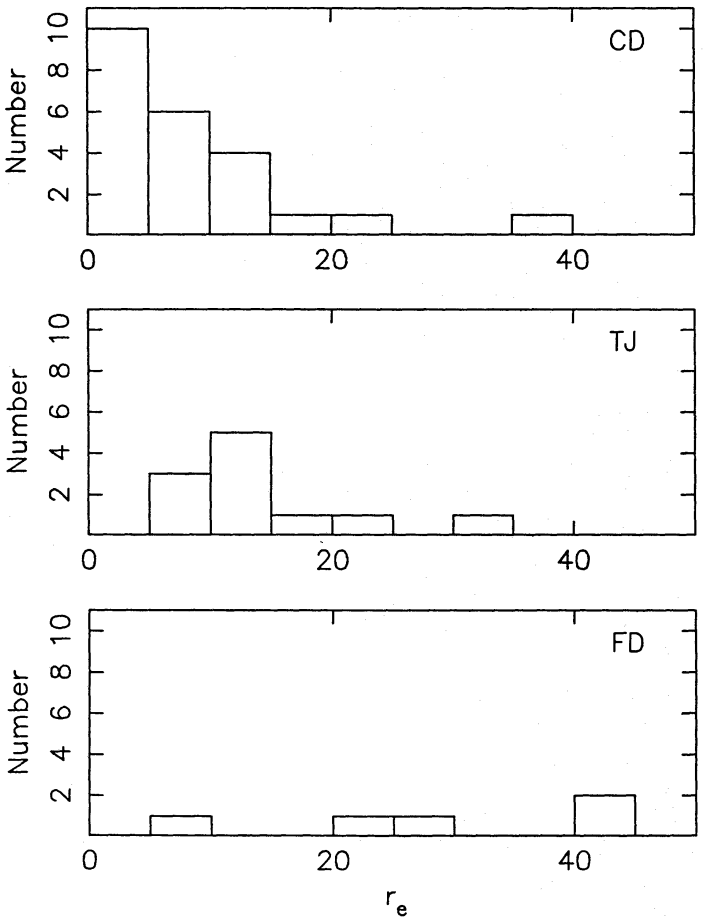

Figure 11. Histograms of de Vaucouleurs' r_e for CD, TJ and FD sources.

($M_{24.5} = -21.9$; Dressler 1978; Luggar 1986). They are certainly much fainter than the first-rank galaxies in rich clusters which Dressler (1978) finds are typically two magnitudes brighter. They also fit $r^{1/4}$ laws quite well, as do most other elliptical galaxies. Thus, photometrically CD radio sources seem to be associated with relatively common galaxies, not the very brightest galaxies in the Universe.

5.2 TJ AND FD PARENT GALAXIES

Surprisingly, the TJ and FD sources, some of which are of much lower luminosity than the CDs, are associated with the brighter galaxies. In general they are also larger and have flatter light distributions. Thus it seems fair to characterize them as D or cD galaxies. In this sample, we have generally avoided radio sources in the centres of rich clusters. We will discuss these galaxies more thoroughly in another paper (Owen & White, paper II in preparation). When we include the rich cluster sources, this conclusion becomes much stronger. But even our galaxies which live only in poor clusters show the trend toward D or cD structure. The TJ and FD galaxies seem to occupy the absolute magnitude range between M^* and the first-rank cluster galaxies.

5.3 EXCEPTIONS

The correlation, of course, is not perfect. First, our data are limited to the range of radio luminosity between 10^{24} and about 3×10^{26} W Hz^{-1} at 1400 MHz. At higher luminosities

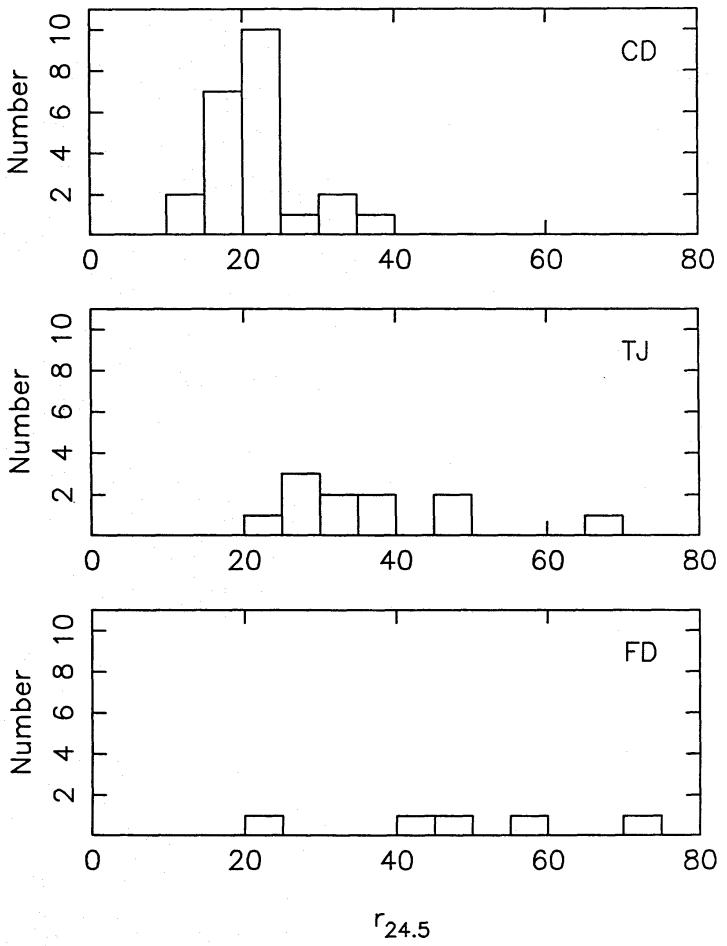

Figure 12. Histograms of $r_{24.5}$ for CD, TJ and FD sources.

most of the objects are at redshifts beyond our redshift cutoff of 0.2. Cygnus A appears to belong to a brighter galaxy, but the situation is complicated by its low galactic latitude and its binary or triple nature (Thompson 1984). Below 10^{24} W Hz^{-1}, our limited data on NGC 5141 and 5490 plus the large number of such sources suggest that the galaxies are fainter, but the radio sources are often also smaller and we may be dealing with different physical questions (e.g. the physics of the galaxy's interstellar medium rather than the intergalactic medium).

The sources in our sample which did not fit the correlation very well also deserve some comment. 3C219 is the brightest classical double source and is also in a confused part of a Zwicky cluster. It is not clear that we are measuring its properties or the overlapping brightness of about six galaxies near the cluster centre. 3C236 also sits at the high end of the size and luminosity distribution for CDs; but it is the largest known radio galaxy by almost a factor of three. DA240 stands out as being fainter than the other FD galaxies, but it is also much larger than any of the other galaxies included in the sample. Further studies are needed to define the relationship of the radio structure to the associated galaxies.

5.4 ABNORMAL STRUCTURES

Heckman *et al.* (1986) report that one-quarter to one-third of radio galaxies with $L \geqslant 3 \times 10^{25}$ W Hz^{-1} are strongly 'peculiar'. We do not find such a strong effect; only one galaxy in the

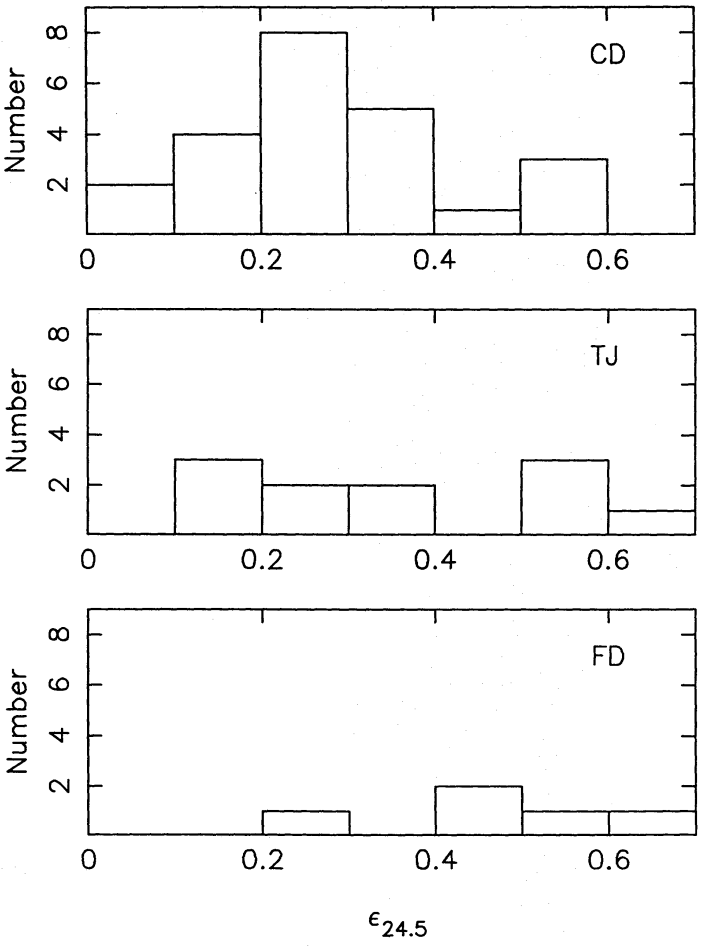

Figure 13. Histograms of $\epsilon_{24.5}$ for CD, TJ and FD sources.

sample which has been analysed statistically is clearly peculiar: as reported by Heckman *et al.*, 3C293 shows a variety of unusual structures which may, in part, have been caused by a tidal interaction. Its bent radio structure may also result from the interaction. One other object in our sample, 3C120, which was excluded because it is core-dominated, shows peculiar optical structure (Arp 1975). Our CCD frame clearly reveals the structures reported by Heckman *et al.* and others. 3C321, another object reported by Heckman *et al.* as peculiar, has a 'tidal' tail on our frame, but it has been excluded from our sample because it lies too near to a bright star. Two other objects reported by Heckman *et al.*, 3C33 and 227, showed no optical peculiarities on our broadband images. The 3C227 structures are seen mainly in narrowband images so it is not surprising that we do not see anything. 3C33 is reported by Simkin & Michel (1986) to show a number of peculiarities seen mainly in an r–i colour map. We see none of these features in our deep R frame, nor the change in isophotal position angle at about 4 arcsec from the nucleus.

Our point is not that the features reported by Heckman *et al.* are not present; only that for galaxies in our sample they are often very faint. For example, the light distribution for 3C33 is well described by an $r^{1/4}$ law and the peculiar features do not strongly perturb the overall structure. Also, many of the objects reported as peculiar by Heckman *et al.* are core-dominated in the radio; some are classified as quasars. They are not well represented in our sample.

Our conclusion is that judgment should be reserved on the importance of the peculiar features. Even in Heckman *et al.*, they represent only a fraction of the total sample. Our

knowledge of the occurrence of peculiar features in field galaxies is poor, at present, and there is no common pattern to the peculiarities. We do know that nuclear emission lines are almost always present in high-luminosity radio galaxies and that sometimes the regions are extended. Further work is therefore necessary before we can draw any major conclusions about the importance of these features to radio galaxy evolution.

5.5 ENVIRONMENT

Studies of the clustering environment of FR I and FR II sources (e.g. Longair & Seldner 1979; Stocke 1979; Lilly & Prestage 1987; Prestage & Peacock 1988) concluded that the FR II sources occur in less dense regions of galaxy clustering than the FR I sources. Lilly & Prestage further conclude that the numbers of close companions or 'multiple nuclei' found for their FR II galaxies are consistent with the number of galaxies expected to be randomly projected on the image of the parent radio galaxy. We have not done detailed galaxy counts for the regions around our sources but from inspection of our images it appears that the CD galaxies are normally in regions of poor clustering, that is the density of galaxies near the radio sources is higher than average but not as high as in the centre of a typical Abell cluster.

X-ray observations (e.g. Feigelson & Berg 1983; Fabbiano *et al.* 1984; Miller *et al.* 1985) show that FR I sources tend to be surrounded by regions of strong X-ray emission, while FR II sources are usually associated with much weaker X-ray sources. This also is consistent with a poor clustering environment for FR II sources.

5.6 A GENERAL PICTURE

The picture which emerges from this study is that sources which we have classified as Classical Doubles (FR II) are generally found in elliptical galaxies with absolute magnitudes approximately equal to M^*. They are normally found in regions of poor clustering. They almost always have nuclear emission lines and may have a more extended region of line emission (Hine & Longair 1979). Also in some cases there is a nuclear continuum source, which is probably non-thermal. The broadband photometric light profiles outside the unresolved nucleus look very much like those of canonical elliptical galaxies. Thus, except for the nucleus and in some cases of extended line emission, the parent galaxies of these powerful radio sources look like commonplace elliptical galaxies.

All lifetime estimates for the Classical Double radio sources are short compared with the lifetime of the galaxy (e.g. Alexander & Leahy 1987); the radiative time-scale for the emission-line gas is also short and the radiating gas needs to be restimulated by activity in the galaxy on an even shorter time-scale. Thus, as far as we can tell, the Classical Double phenomenon is a transient one. It could happen to all M^* ellipticals at some phase in their existence, possibly many times.

On the other hand, the generally less luminous and much more numerous Twin Jet sources are usually associated with brighter, bigger galaxies often in rich clusters and with extreme X-ray emitting gas. They often have D-type envelopes and show relatively little line emission, although our study shows that they are not always at the centres of Abell-type clusters. Fat Double sources seem to occur more rarely but to be associated with similar galaxies and may be just another manifestation of the FR I class.

Classical Double sources are frequently interpreted in terms of supersonic flows, in which the velocity of advance of the head of the jet through the external medium may approach 0.1 c. (e.g. Norman & Winkler 1985; Begelman, Blandford & Rees 1984; Williams 1985). On the other hand, various authors (e.g. Bicknell 1986; Eilek *et al.* 1984) have suggested that Twin Jet

sources seem most easily explained by slower, transonic, or subsonic flows. If this is correct, the lifetimes of Twin Jet sources are probably longer since Twin Jet sources often have similar sizes to the Classical Double sources. The larger space density of TJ sources than CDs, together with their association with brighter, rarer galaxies, also suggest a longer lived, more stable evolution.

Thus it seems reasonable that Classical Doubles are bright transients in ordinary galaxies, while Twin Jets and possibly Fat Doubles are much longer-lived, more stable sources in larger, rarer galaxies. It also seems likely that most Classical Doubles do not evolve into Twin Jet sources, although a Classical Double phase could be part of the evolution of Twin Jet sources. (Possibly Cygnus A, 3C295 and 3C219 are of this type.)

6 Conclusions

(i) Classical double radio sources (generally FR II sources) are statistically associated with elliptical galaxies with normal light profiles and absolute magnitudes similar to M^*.

(ii) Twin Jet and Fat Double radio sources (mostly FR I sources) are statistically associated with brighter, larger galaxies with flatter light distributions than most ellipticals. Even in a sample avoiding rich clusters, many could be classified as D or cD.

(iii) These results together with other statistical and physical arguments suggest that Classical Double sources may be transient phenomena in ordinary galaxies, while Twin Jet and possibly Fat Double sources may be longer-lived and thus more stable structures.

Acknowledgments

The authors thank R. Perley, P. Leahy, V. Kapahi, J. Uson and J. Eilek for comments on the paper, J. Shakeshaft for extensive help in revising the text, and M. Cawson for providing us with the GASP photometric reduction system.

References

Alexander, P., 1985. *Mon. Not. R. astr. Soc.*, **213,** 743.
Alexander, P. & Leahy, J. P., 1987. *Mon. Not. R. astr. Soc.*, **225,** 1.
Antonucci, R. R. J., 1985. *Astrophys. J. Suppl.*, **59,** 499.
Arp, H., 1975. *Publs astr. Soc. Pacif.*, **87,** 545.
Barthel, P. D., Schilizzi, R. T., Miley, G. K., Jägers, W. J. & Strom, R. G., 1985. *Astr. Astrophys.*, **148,** 243.
Baum, S. A., Heckman, T., Bridle, A., van Breugel, W. & Miley, G., 1989. *Astrophys. J. Suppl.*, submitted.
Begelman, M. C., Blandford, R. D. & Rees, M. J., 1984. *Rev. Mod. Phys.*, **56,** 255.
Bicknell, G. V., 1986. *Astrophys. J.*, **300,** 591.
Birkinshaw, M., Laing, R. A. & Peacock, J. A., 1981. *Mon. Not. R. astr. Soc.*, **197,** 253.
Bridle, A. H., Fomalont, E. B. & Cornwell, T. J., 1981. *Astrophys. J.*, **86,** 1294.
Bridle, A. H. & Perley, R. A., 1984. *Ann. Rev. Astr. Astrophys.*, **22,** 319.
Burns, J. O. & Christiansen, W. A., 1980. *Nature*, **287,** 208.
Burns, J. O. & Gregory, S. A., 1982. *Astr. J.*, **87,** 1245.
Burns, J. O. & Owen, F. N., 1979. *Astr. J.*, **84,** 1478.
Burns, J. O., Basart, J. P., DeYoung, D. S. & Ghiglia, D. C., 1984. *Astrophys. J.*, **283,** 515.
Burstein, D. & Heiles, C., 1981. *Astr. J.*, **87,** 1165.
Caswell, J. L. & Wills, D., 1967. *Mon. Not. R. astr. Soc.*, **135,** 231.
Colla, G., Fanti, C., Fanti, R., Gioia, I., Lari, C., Lequeux, J., Lucas, R. & Ulrich, M.-H., 1975. *Astr. Astrophys. Suppl.*, **20,** 1.
Cornwell, T. J. & Perley, R. A., 1985. *Physics of Energy Transport in Extragalactic Radio Sources, Proc. of NRAO Workshop No. 9*, p. 39, ed. Bridle, A. H. & Eilek, J. A., NRAO, Green Bank.

Davis, L. E., Cawson, M., Davies, R. L. & Illingworth, G., 1985. *Astr. J.*, **90,** 169.
Demoulin, M.-H., 1970. *Astrophys. J.*, **160,** L79.
de Ruiter, H., Parma, P., Fanti, C. & Fanti, R., 1986. *Astr. Astrophys. Suppl.*, **65,** 111.
Dreher, J. W. & Feigelson, E. D., 1984. *Nature*, **308,** 43.
Dressler, A., 1978. *Astrophys. J.*, **223,** 765.
Eilek, J. A., Burns, J. O., O'Dea, C. P. & Owen, F. N., 1984. *Astrophys. J.*, **278,** 37.
Fabbiano, G., Miller, L., Trinchieri, G., Longair, M. S. & Elvis, M., 1984. *Astrophys. J.*, **277,** 115.
Fanaroff, B. L. & Riley, J. M., 1974. *Mon. Not. R. astr. Soc.*, **167,** 31.
Fanti, C., Fanti, R., de Ruiter, H. R. & Parma, P., 1986. *Astr. Astrophys. Suppl.*, **65,** 145.
Fanti, R., Gioia, I., Lari, C., Lequeux, J. & Lucas, R., 1973. *Astr. Astrophys.*, **24,** 69.
Fanti, R., Gioia, I., Lari, C. & Ulrich, M.-H., 1978. *Astr. Astrophys. Suppl.*, **34,** 341.
Fanti, R., Lari, C., Parma, P., Bridle, A. H., Ekers, R. D. & Fomalont, E. B., 1982. *Astr. Astrophys.*, **110,** 169.
Feigelson, E. D. & Berg, C. J., 1983. *Astrophys. J.*, **269,** 400.
Fomalont, E. B., Bridle, A. H. & Willis, A. G., 1980. *Astrophys. J.*, **237,** 418.
Griffin, R. F., 1963. *Astr. J.*, **68,** 421.
Gunn, J. E. & Oke, J. B., 1975. *Astrophys. J.*, **195,** 255.
Gunn, J. E., Hoessel, J. G., Westphal, J. A., Perryman, M. A. C. & Longair, M. S., 1981. *Mon. Not. R. astr. Soc.*, **194,** 111.
Heckman, T. M., Smith, E. P., Baum, S. A., van Breugel, W. J. M., Miley, G. K., Illingworth, G. D., Bothun, G. D. & Balick, B., 1986. *Astrophys. J.*, **311,** 526.
Hine, R. G. & Longair, M. S., 1979. *Mon. Not. R. astr. Soc.*, **188,** 111.
Jenkins, C. J., 1982. *Mon. Not. R. astr. Soc.*, **200,** 705.
Jenkins, C. J., Pooley, G. G. & Riley, J. M., 1977. *Mon. Not. R. astr. Soc.*, **84,** 61.
Kron, R. G., Koo, D. C. & Windhorst, R. A., 1985. *Astr. Astrophys.*, **146,** 38.
Laing, R. A., 1981. *Mon. Not. R. astr. Soc.*, **195,** 261.
Laing, R. A., Riley, J. M. & Longair, M. S., 1983. *Mon. Not. R. astr. Soc.*, **204,** 151.
Landolt, A., 1983. *Astr. J.*, **88,** 439.
Leahy, J. P. & Williams, A. G., 1984. *Mon. Not. R. astr. Soc.*, **210,** 929.
Lilly, S. J. & Prestage, R. M., 1987. *Mon. Not. R. astr. Soc.*, **225,** 531.
Lilly, S. J., McClean, I. S. & Longair, M. S., 1984. *Mon. Not. R. astr. Soc.*, **209,** 401.
Linfield, R. & Perley, R. A., 1984. *Astrophys. J.*, **279,** 60.
Longair, M. S. & Gunn, J. E., 1975. *Mon. Not. R. astr. Soc.*, **170,** 121.
Longair, M. S. & Seldner, M., 1979. *Mon. Not. R. astr. Soc.*, **189,** 433.
Luggar, P. M., 1986. *Astrophys. J.*, **303,** 535.
McCarthy, P. J., van Breugel, W., Spinrad, H. & Djorgovski, S., 1987. *Astrophys. J.*, **321,** L29.
Mathews, T. A., Morgan, W. W. & Schmidt, M., 1964. *Astrophys. J.*, **140,** 35.
Mayer, C. J., 1979. *Mon. Not. R. astr. Soc.*, **186,** 99.
Miller, L., 1985. *Mon. Not. R. astr. Soc.*, **215,** 773.
Miller, L., Longair, M. S., Fabbiano, G., Trinchieri, G. & Elvis, M., 1985. *Mon. Not. R. astr. Soc.*, **215,** 799.
Morgan, W. W., 1958. *Publs astr. Soc. Pacif.*, **70,** 364.
Norman, M. L. & Winkler, K.-H. A., 1985. *Los Alamos Science*, **12,** 37.
Parma, P., 1982. *Extragalactic Radio Sources, Proc. IAU Symp. No. 97,* p. 193, ed. Heeschen, D. S. & Wade, C. M., Reidel, Dordrecht.
Perley, R. A., Dreher, J. W. & Cowan, J. J., 1984. *Astrophys. J.*, **285,** 235.
Perley, R. A., Bridle, A. H., Willis, A. G. & Fomalont, E. B., 1980. *Astr. J.*, **85,** 499.
Prestage, R. M. & Peacock, J. A., 1988. *Mon. Not. R. astr. Soc.*, **230,** 131.
Rudnick, L. & Owen, F. N., 1977. *Astr. J.*, **82,** 1.
Sandage, A., 1972. *Astrophys. J.*, **173,** 485.
Sandage, A., 1973. *Astrophys. J.*, **183,** 711.
Sansom, A. E., Danziger, I. J., Ekers, R. D., Fosbury, R. A. E., Goss, W. M., Monk, A. S., Shaver, P. A., Sparks, W. B. & Wall, J. V., 1987. *Mon. Not. R. astr. Soc.*, **229,** 15.
Schweizer, F., 1981. *Astr. J.*, **86,** 662.
Simkin, S. A. & Ekers, R. D., 1983. *Astrophys. J.*, **265,** 85.
Simkin, S. M. & Michel, A., 1986. *Astrophys. J.*, **300,** L5.
Stocke, J., 1979. *Astrophys. J.*, **230,** 40.
Thompson, L. A., 1984. *Astrophys. J.*, **279,** L47.
Ulvestad, J. S. & Johnston, K. J., 1984. *Astr. J.*, **89,** 189.
Waggett, P. C., Warner, P. J. & Baldwin, J. E., 1977. *Mon. Not. R. astr. Soc.*, **181,** 465.

Walker, R. C., Benson, J. M. & Unwin, S. C., 1987. *Astrophys. J.*, **316,** 546.
Williams, A. G., 1985. *PhD thesis*, Cambridge University.
Willis, A. G. & Strom, R. G., 1978. *Astr. Astrophys.*, **62,** 375.
Willis, A. G., Strom, R. G. & Wilson, A. S., 1974. *Nature*, **250,** 625.
Wyndham, J. D., 1966. *Astrophys. J.*, **144,** 459.